Published in final edited form as:
Chem Commun (Camb). 2009 November 14; (42): 6329–6338. doi:10.1039/b911064j.

Discovery and early development of squaraine rotaxanes

Jeremiah J. Gassensmith, **Jeffrey M. Baumes**, and **Bradley D. Smith**
Department of Chemistry and Biochemistry, University of Notre Dame, Notre Dame, IN, 46556, USA.

Abstract

The chemical and photophysical properties of a fluorescent squaraine dye are greatly enhanced when it is mechanically encapsulated inside a tetralactam macrocycle. This feature article describes the synthesis, structure, and photophysical performance of first-generation squaraine rotaxanes, and shows how they can be used as fluorescent imaging probes and chemosensors.

Introduction

The 2008 Nobel Prize was awarded for the discovery and development of the green fluorescent protein (GFP).[1] The story is an inspiring tale of hard work, serendipity, technical brilliance, skillful molecular design, and insightful analytical reasoning.[2] The famous ribbon structure in Fig. 1 shows how the single stranded protein folds up into an 11-stranded beta barrel structure with the chromophore-containing section of the strand threaded through the center.[3] The surrounding barrel plays a crucial role protecting the chromophore from chemical degradation and fluorescence quenching.[4] GFP can be viewed as a biological model for chemists who are pursuing encapsulation strategies to improve the performance of organic dyes.[5] We have contributed to this emerging research topic by developing squaraine rotaxanes. Our discovery of squaraine rotaxanes was due to the fortuitous combination of several factors. In the middle of 2004, one of us (BDS) heard a lecture from Professor David Leigh who described his remarkable clipping method for rotaxane synthesis.[6] During the lecture he noted that the method was quite promiscuous with regard to the structure of the thread component, due in part to the flexibility of the surrounding macrocycle.[7] A few months later a new postdoctoral associate, Dr Easwaran Arunkumar, started in the Smith group with expertise in squaraine dyes.[8] Squaraines have an internal donor–acceptor–donor structure as represented by the resonance contributors shown in Fig. 2.[9] They are intensely colored fluorescent dyes that absorb and emit in the deep-red and near-infrared wavelengths.[8] This is a valuable wavelength region for many types of imaging applications, however, squaraines have potential limitations in biological environments. Under aggregation conditions they are not fluorescent and they are susceptible to attack by strong nucleophiles. It occurred to us that both problems would be solved simultaneously if the dye was protected inside a container molecule and we were particularly intrigued by papers from the group of Anderson and co-workers who described examples of acetylene, azo, and cyanine dyes encapsulated by cyclophanes and cyclodextrins.[10–12] Thus, in September 2004 we attempted to trap a squaraine dye inside a Leigh-type tetralactam macrocycle. Success was immediate and three months later we submitted our first communication.[13]

smith.115@nd.edu; Fax: +1 5746316652; Tel: +1 5746318632.

Synthesis

Symmetrical squaraine dyes are prepared in one step on a half-gram scale by heating, under azeotrope distillation conditions, two equivalents of the appropriate aniline derivative with squaric acid (Scheme 1).[14] Unsymmetrical squaraines are made in two steps, by first treating an aniline derivative with squaryl dichloride to give a stable semi-squaraine intermediate, which is then heated with a second aniline derivative to give the unsymmetrical squaraine. These dye-forming reactions tolerate aniline derivatives containing weakly nucleophilic functional groups including alcohol, carboxylic acid, and ester groups.

Squaraine rotaxanes are assembled by two general synthetic methods, clipping and capping.[15] The differences in these methods, illustrated in Fig. 3, are distinguished by the order in which the components are assembled. In the case of clipping, the thread component is fully formed and serves as a template for the macrocyclization reaction. Capping, on the other hand, attaches bulky stopper groups to the ends of a pseudorotaxane complex that is formed by reversible, non-covalent self-assembly.[16] The technical simplicity of the Leigh-type clipping reaction, and the commercial availability of reactants, makes it an attractive starting option for rotaxane synthesis. Shown in Scheme 2 are the first reactions we performed to make squaraine rotaxanes with tetralactam macrocycles.[13] The syntheses involves simultaneous slow addition of separate solutions of the appropriate diacid dichloride and *p*-xylylenediamine under pseudo-dilution conditions to a stirring, room temperature solution of squaraine dye in anhydrous chloroform. The reactions produce squaraine rotaxanes **2** in reproducible yields of 20–35% after purification by silica gel column chromatography. Although the synthetic yields are modest, the assembly process is notable because it captures five components in a single step.

We assumed from previous mechanistic work[6] that the key template interaction favoring rotaxane formation was hydrogen bonding of the immediate acyclic precursor of the macrocycle to the squaraine oxygens (top of Fig. 3). This raised the possibility that other macrocycle architectures with the same pattern of NH residues may also form squaraine rotaxanes.[17] Therefore, we investigated the outcome of "reversing" the aromatic electron density in the surrounding macrocycle. A structural isomer was created by switching the locations of the electron rich xylylene and electron-deficient phthaloyl subunits. In this case, the Leigh-type clipping reaction with *p*-phthaloyl chloride and *m*-xylylenediamine produced the isomeric rotaxane **3** but in only 9% yield.[18] The lower yield suggests that hydrogen bonding is important for the template effect but that the rotaxane assembly process is optimal when the surrounding macrocycle contains electron rich *p*-xylylene subunits as the side-walls.

To employ squaraine rotaxanes as versatile fluorescent molecular probes for optical bioimaging, it is necessary to develop robust, high-yielding synthetic methods for bioconjugation. As unencapsulated molecules in solution, squaraine dyes react with strongly nucleophilic functional groups and in solution, they slowly decompose in the presence of amides and alcohols. In contrast, squaraine rotaxanes exhibit good solubility and very high chemical stability. They are compatible with most electrophiles and nucleophiles, and they are excellent building blocks for further synthetic elaboration, as long as the rotaxane structure stays intact during the synthesis. Our first-generation squaraine rotaxanes employed large *N*,*N*′-dibenzylamine stopper groups to ensure unambiguously that rotaxane unthreading did not occur, but over the past few years we have discovered that unthreading is not a significant problem even with small stopper groups. For example, we have prepared and studied the various rotaxanes shown in Fig. 4 and found that all of them are mechanically stable in chloroform solvent even at elevated temperatures.[19] Squaraine rotaxane unthreading is most likely to occur in polar aprotic solvents, such as DMSO or DMF, that effectively disrupt hydrogen bonds and also minimize attractive dispersion interactions.[20] However, it is notable that unthreading is inhibited by the presence of water because the hydrophobic effect favors

the rotaxane's aromatic stacking. Therefore, synthetic reactions that modify the structures of mechanically bonded squaraine rotaxanes are best conducted in weakly polar organic solvents like chloroform or otherwise highly polar protic solvents like water.

To achieve bioconjugation, we have developed effective amide bond coupling methods. A squaraine rotaxane that has an appended carboxylic acid group can be activated for covalent reaction with a targeting ligand that has an amine group. For example, the reaction in Scheme 3 connects an asymmetric squaraine rotaxane to a bacteria targeting unit that comprises two zinc coordinated 2,2′-dipicolylamine-(bis-ZnDPA) groups.[21] The copper catalyzed azide-alkyne cycloaddition or click reaction is another conjugation method that works well with squaraine rotaxanes. Click chemistry readily connects a squaraine rotaxane that has an appended alkyne group with a targeting ligand that has an azide group. The use of click chemistry to make bioimaging probes is attractive for several reasons, the synthetic yields are very high, the reaction is perfectly atom economical, and the triazole linkages resist cleavage by common hydrolytic enzymes.[22]

As mentioned above, squaraine rotaxanes can be prepared by covalent capping of the ends of a pseudorotaxane complex with stopper groups. The original Leigh-type macrocycle with *p*-xylylene side-walls is incompatible with this methodology due to its inherent insolubility in organic solvents.[23] However, we have discovered that macrocycle family **5**, an anthracene variant of the Leigh-type tetralactam, possesses good organic solubility and a very high encapsulation affinity for squaraine dyes.[24] As shown in Scheme 4, ‘‘clicked capping’’ reactions with these anthracene-derived macrocycles produce squaraine rotaxanes, such as **6**, in nearly quantitative yield.[25]

Structure

It is relatively easy to obtain squaraine rotaxanes as single crystals that are suitable for analysis by X-ray diffraction. The first two crystal structures that we solved showed the macrocycles in chair conformations with bifurcated hydrogen bonding between the macrocycle 1,3-dicarboxamide moieties and the squaraine oxygens (Fig. 5). The 2,6-pyridine dicarboxamide-containing macrocycle (hereafter referred to as the pyridyl-containing macrocycle) in rotaxane **2a** wraps more tightly around the squaraine thread than the isophthalamide-containing macrocycle in rotaxane **2b**. This is reflected by a shorter centroid-to-centroid distance between the macrocycle's parallel xylylene units (6.61 Å compared to 7.05 Å), and also by a lower degree of macrocycle conformational disorder in the solid-state. The reason for the difference is internal hydrogen bonding between the pyridyl nitrogen and the two adjacent NH residues which contracts the macrocycle size and reduces flexibility.[26]

Subsequently we obtained crystal structures of several other squaraine rotaxanes and discovered a much wider array of macrocycle conformational diversity.[27] In particular, squaraine rotaxanes with pyridyl-containing macrocycles, such as **7**, have a propensity to adopt boat conformations in the solid-state (Fig. 6). Interestingly, these boat-conformation macrocycles retain the intercomponent hydrogen bonding but the macrocycle is not located directly over the center of the squaraine thread. In solution, there is no evidence that these asymmetric boat conformations are predominant, because the ^{1}H NMR spectral patterns are symmetric even at very low temperature. Most likely, the rotaxane macrocycles exist as a rapidly exchanging equilibrium of boat and chair conformations that have similar energies. The X-ray structures provide snapshots of this conformational exchange, and indicate that as the macrocycles flip between chair and boat conformations they undergo a transverse oscillation of their positions relative to the center of the encapsulated squaraine thread (Fig. 7). In addition to chair–boat conformational exchange it is likely that the macrocycle pirouettes

around the squaraine thread,[6] but the molecular symmetry of the molecules does not allow this motion to be detected by ^{1}H NMR.

Shown in Fig. 8 is a crystal structure of a pseudorotaxane comprising *N*,*N*′-tetramethylsquaraine encapsulated inside the anthracene-derived macrocycle **5a**.[28] As expected the two anthracene walls stack against the squaraine dye and the anthracene centroid-to-centroid distance is 6.8 Å. Also expected are the bifurcated hydrogen bonds between the amide NH residues and the squaraine oxygens, as well as the internal hydrogen bonding network that is characteristic of the 2,6-pyridine dicarboxamide moiety. The macrocyclic conformation is almost planar, but there appears to be some degree of flexibility as we have obtained unpublished structures from different crystals with the macrocycle in a chair-like conformation.

Photophysical properties and chemical stability

Over the years, squaraine dyes have been investigated for potential applications in many photonic based technologies, such as photoconductive materials, optical data storage, solar energy capture, non-linear optics, chemical sensors, and imaging probes.[9] The electronic structures of the S_0 and S_1 states have been examined theoretically, and they are thought to be intramolecular charge transfer states.[29] The anilino rings and carbonyl oxygens are donors to the electron-deficient C_4O_2 core and the charge transfer is primarily localized to this core. Because of this localization, the electronic transition is a narrow absorption band and there is only a small structure substituent effect on the observed absorption maxima. As a result, asymmetric squaraine dyes have similar quantum yields and similar absorption/emission bandwidths as symmetric analogues. The quantum yields are typically quite high in organic solvents, but they are decreased in polar protic solvents.[30]

Not unexpectedly, the photophysical properties of a squaraine dye are altered when the dye is encapsulated as the thread component inside a tetralactam macrocycle. The effect is macrocycle dependent. The original Leigh-type macrocycles in **2** with *p*-xylylene side-walls induce a 10–20 nm red-shift in absorption/emission wavelengths. The effect on fluorescence quantum yield is varied; rotaxane **2a** with a pyridyl-containing macrocycle exhibits a slighter higher quantum yield than the parent dye, whereas the quantum yield of rotaxane **2b** with a isophthalamide-containing macrocycle is lower by a factor of three (Table 1).

Encapsulation inside the anthracene-containing macrocycle **5** leads to a more substantial 20–40 nm red-shift in absorption/emission wavelengths.[28] This red-shift effect was recently studied by Jacquemin and co-workers using time-dependent density functional theory.[31] The team concluded that the shift is due to two effects, geometric deformations of the squaraine brought on by the encapsulation and stabilization of the squaraine excited state by electronic reorganization of the surrounding macrocycle. Although the squaraine fluorescence quantum yield was observed to decrease slightly upon encapsulation inside **5a**, there is a strong insulation effect against solvent induced quenching due to the deep encapsulation inside the macrocycle. For example, the quantum yield of a normal squaraine dye drops by about a factor of 10 as the solvent is changed incrementally from pure chloroform to pure methanol. With *p*-xylylene-containing rotaxane **2a** the squaraine quantum yield decreases by a factor of 3, whereas it is lowered by only 20% when the encapsulating macrocycle is the anthracene-containing **5a**.[28] This trend is reminiscent of the dramatic increase in quantum yield that is gained by deep encapsulation of the GFP chromophore inside the surrounding barrel (Fig. 1).

Dye encapsulation helps eliminate another drawback of squaraine dyes, namely, the tendency to form non-fluorescent aggregates in aqueous solution. When aggregated or packed in the solid-state, squaraines exhibit broad absorption bands, a useful attribute for applications like solar collection and xerographic devices, but an undesired feature for bioimaging. This

broadening effect is demonstrated in Fig. 9 which shows that the sharp squaraine absorption in DMSO is lost when the dye is aggregated in 1 : 1 DMSO–water. The H- and J-aggregates that are formed under these conditions lead to blue- and red-shifted bands, respectively.[32] In contrast, the absorption bands of the corresponding squaraine rotaxane **2a** are not broadened, even under the strongly aggregating conditions of 1 : 9 DMSO–water. This suggests that when squaraine rotaxanes are aggregated, the encapsulated dye components are prevented from getting close enough to engage in effective interchromophore energy transfer.

Ground-state squaraines are susceptible to attack at the electrophilic C_4O_2 core by strong biological nucleophiles such as thiols, primary amines, and even water.[33] Reversible covalent addition occurs at the positions indicated by the arrows in Fig. 10. Encapsulation inside a tetralactam macrocycle provides substantial steric protection that is easily demonstrated by color fading experiments. For example, in aqueous solution, a neutral squaraine dye loses its color within a couple of days, whereas the corresponding squaraine rotaxane retains its color for many weeks. Furthermore, squaraine rotaxane are stable for several hours at extreme pH values of 2 and 12. Shown in Fig. 11 is a visual comparison of the different reactivities with thiols. Addition of excess cysteine to a vial containing free squaraine dye leads to complete loss of the blue color in five minutes, whereas the same treatment of a squaraine rotaxane does not induce any change in color intensity. The steric protection is macrocycle dependent. The pyridyl-containing macrocycle in **2a** is more effective at blocking cysteine attack than the isophthalmide-containing macrocycle in **2b** and the isomeric macrocycle in **3**. This agrees with the dynamic picture that the pyridyl-containing macrocycle is more tightly wrapped around the squaraine thread than the other two macrocycles, offering fewer transient opportunities for nucleophilic attack at the electrophilic squaraine core.

Another major reactivity problem with fluorescent organic dyes is photobleaching. Squaraines do not undergo rapid photobleaching for several reasons. Singlet to triplet intersystem crossing is quite inefficient with non-halogenated squaraines,[34] thus irradiation produces relatively low amounts of reactive oxygen species (ROS), which is a major source of photobleaching. In addition, squaraines do not have reactive carbon–carbon double bonds and therefore they react slowly with any ROS that is formed.[35] The Leigh-type macrocycles also have low reactivity with ROS, and thus it is not surprising that squaraine rotaxanes have very high resistance to photobleaching. The remarkable photostability was demonstrated by studying the tetra(iodo)-substituted squaraine rotaxane **7**.[36] The heavy iodine atoms promote intersystem crossing from the squaraine excited singlet state and subsequent triplet energy transfer to create large amounts of ROS, including singlet oxygen.[37] However, squaraine rotaxane **7** does not react with the ROS and therefore does not undergo photobleaching. The results of this study suggest that halogenated squaraine rotaxanes are likely to be very useful as research tools for studies of photodynamic therapy. As inert oxygen photosensitizers, they can create known amounts of singlet oxygen in a controlled manner and without the complication introduced by photosensitizer decomposition.

Squaraine rotaxanes as fluorescent imaging probes and chemosensors

Biomedical science would broadly benefit from an improved suite of highly stable and very bright fluorescent dyes that emit at suitably spaced wavelengths between 400 nm to 800 nm.[38] These dyes can be attached to targeting molecules, like antibodies and DNA, to make fluorescent probes that can be distinguished by microscopes, microarray devices, and imaging stations that are equipped with different observation filter sets.[39] Many imaging systems split the filter sets into five channels; blue (425–480 nm, *e.g.* coumarin), green (510–570 nm, *e.g.* fluorescein), red (570–630 nm, *e.g.* rhodamine), deep-red (650–740 nm, *e.g.* Cy5) and near-infrared (770–850 nm, *e.g.* Cy7).[40] The bis(anilino) squaraine rotaxanes in this article emit in the deep-red channel (650–740 nm, *e.g.* Cy5).[8] This wavelength is very versatile because it

can be seen by the naked eye as a red color but the background autofluorescence from other biomolecules is low. The deep-red channel can be excited by cheap lasers, and there are specific rapid scanning and high performance imaging technologies that take advantage of the intense laser light (*e.g.*, ultrahigh resolution cell microscopy, intravital microscopy, and microarray scanning). Furthermore, deep-red light can potentially penetrate several centimetres through skin and tissue;[41] thus appropriately designed fluorescent probes can be used for whole-body optical imaging of live animals.[42] At present, the most common fluorescent red and near-infrared dyes for bioimaging are cyanine dyes (Cy5, Cy5.5, Cy7) and their derivatives.[43] However, cyanine dyes are far from perfect and have several limitations such as moderate to poor photostability, undesired reactivity with nucleophiles, and propensity to self-quench.[44] The need for improved red and near-infrared fluorescent dyes is well-recognized by many research groups around the world.[45]

In 2007, we published a comparative study that highlighted the performance advantages of squaraine rotaxanes over Cy5.[21] We prepared and evaluated the squaraine rotaxane probes **4** and **8** and compared them to the Cy5 probe **9**. Each probe has essentially the same absorption/emission maxima, and each has appended bis-ZnDPA groups which are known to target the surfaces of bacterial cells (Fig. 12).[46] To measure photostability, separate samples of *Escherichia coli* were stained with the three probes and the samples were irradiated continuously with the light source in an epifluorescence microscope. The subsequent fading of fluorescent image over time produced the following photobleaching half-lives: 1080 s for **8**, 197 s for **4**, and 11 s for Cy5 **9**. Thus, direct comparison between squaraine rotaxane **4** and cyanine **9** indicates that the squaraine rotaxane is 20 times more photostable. The symmetric squaraine rotaxane probe **8**, which has two bis-ZnDPA units, is able to associate more strongly with the bacterial surface and has a lower rate of signal loss due to probe dissociation. It is an exceptionally stable, high-affinity bacterial imaging probe and can be used to conduct real-time imaging experiments that were previously impossible. For example, Fig. 13 shows a montage of images from a 30-minute movie that monitors binary fission of *E. coli* cells stained with **8**. These images of healthy, living cells emphasize not just the photostability of the probe but also the low phototoxicity of squaraine rotaxanes. The potential for *in vivo* imaging was demonstrated in the following way: separate samples of *E. coli* and *Staphylococcus aureus* were stained with rotaxane **8** and then injected subcutaneously into the upper rear legs of a living nude mouse. The entire animal was irradiated with light filtered to be 625 ± 40 nm and an image of fluorescent emission at 670 ± 20 nm was collected by a charged coupled device. The optical image in Fig. 14 shows that both inoculations are very apparent with fluorescence signal intensities that are about 100 times greater than the background fluorescence. Taken together, the imaging data suggest that squaraine rotaxanes can be converted into bright and highly stable deep-red fluorescent probes that should enable a range of new biomedical imaging techniques such as high intensity intravital microscopy, re-usable microarrays, and endoscopic detection of diseases such as cancer and bacterial infection.

There is also recent evidence that squaraine rotaxanes can be developed into fluorescent chemosensors and logic devices that report the presence and concentration of target analytes. Recently, we reported that the well-known tetralactam, **10**, can encapsulate squaraine dyes with modest affinity and partially quench the squaraine fluorescence (Fig. 15).[25] This enabled the construction of a dye displacement process that reports the presence of inorganic anions. Macrocycle **10** is known to strongly bind small anions like chloride and acetate.[47] Thus, addition of these anions as tetrabutylammonium salts to the psuedorotaxane leads to displacement of the squaraine dye and restoration of its fluorescence intensity.

An example of a metal ion sensing is shown in Fig. 16. The crown ether derived macrocycle **11** only binds a squaraine dye when Na^+ ions are present in the solution.[48] Two Na^+ ions bridge the squaraine and the crown ether oxygens, an inclusion process that enhances the dye's

fluorescence. Addition of K^+ leads to ejection of the squaraine and the Na^+ ions from the cavity, and a return to lower squaraine fluorescence. This multicomponent assembly system acts like a rudimentary Boolean logic device, where the presence of Na^+ alone causes an increase in fluorescence, but K^+ alone or a Na–K^+ mixture produces no change in signal. It is important to remember that the deep-red squaraine fluorescence is well-suited for operation in biomedical samples, thus next-generation designs of squaraine rotaxane chemosensors have potential for rapid translation as practical devices.

Conclusions

Squaraine rotaxanes are emerging as a promising new family of deep-red fluorescent dyes with extreme brightness and very high stability. Covalent conjugation of squaraine rotaxanes with biological targeting agents produces fluorescent probes that are very effective in various bioimaging applications. The structure of the surrounding macrocycle is a molecular design parameter that can be used to fine-tune the photophysical properties of the encapsulated squaraine dye. Squaraine rotaxanes are an excellent example of how molecular encapsulation can be used to protect and improve the chemical and photophysical attributes of a fluorescent dye. The encapsulation strategy is reminiscent of the process used by GFP to exhibit its extraordinary fluorescent properties. The intrinsic dynamic properties of rotaxanes, especially the capacity to undergo large amplitude shuttling motions, raise the possibility of creating dynamic squaraine rotaxanes that can report recognition-induced translocation processes as red fluorescent signals.

Acknowledgments

This work was supported by the NSF, the NIH, and the University of Notre Dame. We warmly acknowledge the technical expertise and intellectual contributions of all members of the Smith group who have contributed to this ongoing squaraine rotaxane project.

Jeremiah J. Gassensmith

Jeffrey Baumes was born in Binghamton, New York. He received his BS in both Chemical Engineering and Chemistry from Clarkson University in 2006. He has since joined the group of Prof. Bradley Smith at the University of Notre Dame as a PhD student. His research focuses on the development and study of dendritic supra-molecular squaraine rotaxane systems.

Jeffrey Baumes was born in Binghamton, New York. He received his BS in both Chemical Engineering and Chemistry from Clarkson University in 2006. He has since joined the group of Prof. Bradley Smith at the University of Notre Dame as a PhD student. His research focuses on the development and study of dendritic supramolecular squaraine rotaxane systems.

Bradley D. Smith is Emil T. Hofman Professor of Chemistry and Biochemistry and Director of the Notre Dame Integrated Imaging Facility. His research interests are primarily in the field of supramolecular chemistry applied to biological systems. A current topic is the creation of molecular imaging probes for detecting cancer and microbial infections.

Notes and references

1. Miyawaki A. Cell 2008;135:987. [PubMed: 19070562]
2. Nienhaus GU. Angew. Chem., Int. Ed 2008;47:8992.
3. Ormo M, Cubitt AB, Kallio K, Gross LA, Tsien RY, Remington SJ. Science 1996;273:392.
4. Pakhomov A, Martynov VI. Chem. Biol 2008;15:755. [PubMed: 18721746]
5. Arunkumar E, Forbes CC, Smith BD. Eur. J. Org. Chem 2005:4051.
6. a Leigh DA, Murphy A, Smart JP, Slawain AMZ. Angew. Chem., Int. Ed. Engl 1997;36:728. b Gatti FG, Leigh DA, Nepogodiev SA, Slawin AMZ, Teat SJ, Wong JKY. J. Am. Chem. Soc 2001;123:5983. [PubMed: 11414832] c Brancato G, Coutrot F, Leigh DA, Murphy A, Wong JKY, Zerbetto F. Proc. Natl. Acad. Sci. U. S. A 2002;99:4967. [PubMed: 11959948]
7. Clegg W, Gimenez-Saiz C, Leigh DA, Murphy A, Slawin AMZ, Teat SJ. J. Am. Chem. Soc 1999;121:4124.
8. This article focuses bis(anilino squaraines, which are one class of the large family of dyes derived from squaric acid. For examples of other architectures, see: a Ajayaghosh A. Acc. Chem. Res 2005;38:449. [PubMed: 15966711] ; b Ajayaghosh A. Chem. Soc. Rev 2003;32:181. [PubMed: 12875024] ; c Meier H, Dullweber U. J. Org. Chem 1997;62:4821.; d Basheer MC, Santhosh U, Alex S, Thomas KG, Suresh CH, Das S. Tetrahedron 2007;63:1617.; e Oswald B, Patsenker L, Duschl J, Szmacinski H, Wolfbeis OH, Terpetschnig E. Bioconjugate Chem 1999;10:925.; f Emmelius M, Pawlowski G, Vollmann HW. Angew. Chem., Int. Ed. Engl 1989;28:1445.
9. a Law K-Y. Chem. Rev 1993;93:449.b Law, K-Y. Organic Photochemistry. Ramamurthy, V.; Schanze, KS., editors. Marcel Dekker; New York: 1997. p. 519c Das, S.; Thomas, KG.; George, MV. Organic Photochemistry. Ramamurthy, V.; Schanze, KS., editors. Marcel Dekker; New York: 1997. p. 467
10. a Anderson S, Anderson HL. Angew. Chem., Int. Ed. Engl 1996;35:1956. b Anderson S, Claridge TDW, Anderson HL. Angew. Chem., Int. Ed. Engl 1997;36:1310. c Anderson S, Clegg W, Anderson HL. Chem. Commun 1998:2379. d Craig MR, Hutchings MG, Claridge TDW, Anderson HL. Angew. Chem., Int. Ed 2001;40:1071. e Buston JEH, Young JR, Anderson HL. Chem. Commun 2000:905.

11. For examples of steric protection of rotaxane thread components, see: a Parham AH, Windisch B, Vögtle F. Eur. J. Org. Chem 1999:1233.; b Reuter C, Vögtle F. Org. Lett 2000;2:593. [PubMed: 10814386] ; c Ghosh P, Mermagenaand O, Schalley CA. Chem. Commun 2002:2628.; d Oku T, Furusho Y, Takata T. Org. Lett 2003;5:4923. [PubMed: 14682730]
12. For recent examples of dye encapsulation, see: a Park JS, Wilson JN, Hardcastle KI, Bunz UHF, Srinivasarao M. J. Am. Chem. Soc 2006;128:7714. [PubMed: 16771466] ; b Mohanty J, Pal H, Ray AK, Kumar S, Nau WM. ChemPhysChem 2007;8:54. [PubMed: 17171726] ; c Comes M, Marcos MD, Martínez-Máñez R, Millán MC, Ros-Lis JV, Sancenön F, Soto J, Villaescusa LA. Chem.–Eur. J 2006;12:2162.; d Constantin TP, Silva GL, Robertson KL, Hamilton TP, Fague K, Waggoner AS, Armitage BA. Org. Lett 2008;10:1561. [PubMed: 18338898] ; e Yau CMS, Pascu SI, Odom SA, Warren JE, Klotz EJF, Frampton MJ, Williams CC, Coropceanu V, Kuimova MK, Phillips D, Barlow S, Brédas J, Marder SR, Millar V, Anderson HL. Chem. Commun 2008:2897.
13. Arunkumar E, Forbes CC, Noll BC, Smith BD. J. Am. Chem. Soc 2005;127:3288. [PubMed: 15755140]
14. Schmidt H. Synthesis 1980:96.
15. Schalley A, Weilandt T, Bruggemann J, Vögtle F. Top. Curr. Chem 2004;248:141.
16. a Klotz EJF, Claridge TDW, Anderson HL. J. Am. Chem. Soc 2006;128:15374. [PubMed: 17131994] b Hübner GM, Reuter C, Seel C, Vögtle F. Synthesis 2000:103. c Dunnwald T, Jäger R, Vögtle F. Chem.–Eur. J 1997;3:2043.
17. Leigh A, Venturini A, Wilson AJ, Wong JKY, Zerbotto F. Chem.–Eur. J 2004;10:4960.
18. Arunkumar, Fu N, Smith BD. Chem.–Eur. J 2006;12:4684.
19. Fu N, Gassensmith JJ, Smith BD. Supramol. Chem 2009;21:118. [PubMed: 20376290]
20. Wu, Mukhopadhyay P, Chakraborty A, Fettinger JD, Isaacs L. J. Am. Chem. Soc 2004;126:10035. and references therein. [PubMed: 15303878]
21. Johnson JR, Fu N, Arunkumar E, Leevy WM, Gammon ST, Piwinica-Worms D, Smith BD. Angew. Chem., Int. Ed 2007;46:5528.
22. a Sun EY, Josephson L, Weissleder R. Mol. Imaging 2006;5:122. [PubMed: 16954026] b Binder WH, Sachsenhofer R. Macromol. Rapid. Commun 2007;28:15.
23. a Johnston AG, Leigh DA, Murphy A, Smart JP, Deegan MD. J. Am. Chem. Soc 1996;118:10662. b Inoue Y, Kanbara T, Yamamoto T. Tetrahedron Lett 2003;44:5167.
24. Gassensmith JJ, Baumes JM, Eberhard J, Smith BD. Chem. Commun 2009:2517.
25. Gassensmith JJ, Barr L, Baumes JM, Paek A, Nguyen A, Smith BD. Org. Lett 2008;10:3343. [PubMed: 18582079]
26. Affeld GM, Hübner C, Seel C, Schalley CA. Eur. J. Org. Chem 2001:2877. and references therein.
27. Fu N, Baumes JM, Arunkumar E, Noll BC, Smith BD. submitted for publication.
28. Gassensmith JJ, Arunkumar E, Barr L, Baumes JM, DiVittorio KM, Johnson JR, Noll BC, Smith BD. J. Am. Chem. Soc 2007;129:15054. [PubMed: 17994746]
29. Bigelow RW, Freund HJ. Chem. Phys 1986;107:159.
30. Ros-Lis JV, Martinez-Manez R, Sancenon F, Soto J, Spieles M, Rurack K. Chem.–Eur. J 2008;14:10101.
31. Jacquemin D, Perpete EA, Laurent AD, Assfeld X, Adam C. Phys. Chem. Chem. Phys 2009;11:1258. [PubMed: 19209370]
32. a Chen H, Law K-Y, Perlstein J, Whitten DG. J. Am. Chem. Soc 1995;117:7257. b Liang K, Law K-Y, Whitten DG. J. Phys. Chem 1994;98:13379. c Das S, Thomas KG, Thomas KJ, Madhavan V, Liu D, Kamat PV, George MV. J. Phys. Chem 1996;100:17310. d Arun KT, Epe B, Ramaiah D. J. Phys. Chem. B 2002;106:11622.
33. a Ros-Lis JV, Garcia B, Jimenez D, Martinez-Manez R, Sancenon F, Soto J, Gonzalvo F, Valldecabres MC. J. Am. Chem. Soc 2004;126:4064. [PubMed: 15053569] b Ros-Lis JV, Martínez-Máñez R, Soto J. Chem. Commun 2002:2248.
34. Thomas KG, Thomas KJ, Das S, George MV, Liu D, Kamat PV. J. Chem. Soc., Faraday Trans 1996;92:4913–4916.
35. Kamat PV, Das S, Thomas KG, George MV. J. Phys. Chem 1992;96:195.
36. Arunkumar E, Sudeep PK, Kamat KV, Noll B, Smith BD. New J. Chem 2007;31:677.

37. Ramaiah D, Eckert I, Arun KT, Weidenfeller L, Epe B. Photochem. Photobiol., A 2004;79:99.
38. Rao JH, Dragulescu-Andrasi A, Yao HQ. Curr. Opin. Biotechnol 2007;18:17. [PubMed: 17234399]
39. a Shen, X.; Van Wijk, R., editors. Biophotonics: Optical Science and Engineering for the 21st Century. Springer; New York: 2005. b Cox, GC., editor. Optical Imaging Techniques in Cell Biology. CRC Press; Boca Raton: 2007. c Wolfbeis, OS. Fluorescence Methods and Applications: Spectroscopy, Imaging, and Probes. Wiley-Blackwell; New York: 2008.
40. Davis LD, Raines RT. ACS Chem. Biol 2008;3:142. [PubMed: 18355003]
41. Bashkatov N, Genina EA, Kochubey VI, Tuchin VV. J. Phys. D: Appl. Phys 2005;38:2543.
42. Keller PJ, Pampaloni F, Stelzer EH. Curr. Opin. Cell Biol 2006;18:117. [PubMed: 16387486]
43. Mishra A, Behera RK, Behera PK, Mishra BK, Behera GB. Chem. Rev 2000;100:1973. [PubMed: 11749281]
44. a Berlier JE, et al. J. Histochem. Cytochem 2003;51:1699. [PubMed: 14623938] b Kassab K, Photochem J. Photobiol., B 2002;68:15. c Lin YH, Weissleder R, Tung CH. Bioconjugate Chem 2002;13:605. d Li W-R, Wang H, Yang T-X, Zhang H-S. Anal. Bioanal. Chem 2003;377:350. [PubMed: 12898114] e Ye Y, Bloch S, Kao J, Achilefu S. Bioconjugate Chem 2005;16:51. f Zhang Z, Achilefu S. Org. Lett 2004;6:2067. [PubMed: 15176820]
45. For recent examples of new dye syntheses, see: a Niu SL, Ulrich G, Ziessel R, Kiss A, Renard PY, Romieu A. Org. Lett 2009;11:2049. [PubMed: 19379006] ; b Umezawa K, Matsui A, Nakamura Y, Citterio D, Suzuki K. Chem.–Eur. J 2009;15:1096.; c Teo YN, Wilson JN, Kool ET. J. Am. Chem. Soc 2009;131:3923. [PubMed: 19254023] ; d Umezawa K, Nakamura Y, Makino H, Citterio D, Suzuki K. J. Am. Chem. Soc 2008;130:1550. [PubMed: 18193873] ; e Yang Y, Lowry M, Xiangyang X, Escobedo JO, Sibrian-Vazquez M, Wong L, et al. Proc. Natl. Acad. Sci. U. S. A 2008;105:8829. [PubMed: 18579790] ; f Kim SH, Guncher JR, Katzenellenbogen JA. Org. Lett 2008;10:4931. [PubMed: 18841988] ; g Fu MY, Xiao Y, Qian XH, Zhao DF, Xu YF. Chem. Commun 2008:1780.; h Han J, Jose J, Mei E, Burgess K. Angew. Chem., Int. Ed 2007;46:1684.; i Daltrozzo E, Fischer GM, Ehlers AP, Zumbusch A. Angew. Chem., Int. Ed 2007;46:3750.
46. Leevy WM, Johnson JR, Lakshmi C, Morris J, Marquez M, Smith BD. Chem. Commun 2006:1595.
47. a Seel C, Parham AH, Safarowsky O, Hübner GM, Vögtle F. J. Org. Chem 1999;64:7236. b Hübner GM, Gläser J, Seel C, Vögtle F. Angew. Chem., Int. Ed 1999;38:383.
48. Hsueh S-Y, Lai C-C, Liu Y-H, Peng S-M, Chiu S-H. Angew. Chem., Int. Ed 2007;46:2013.

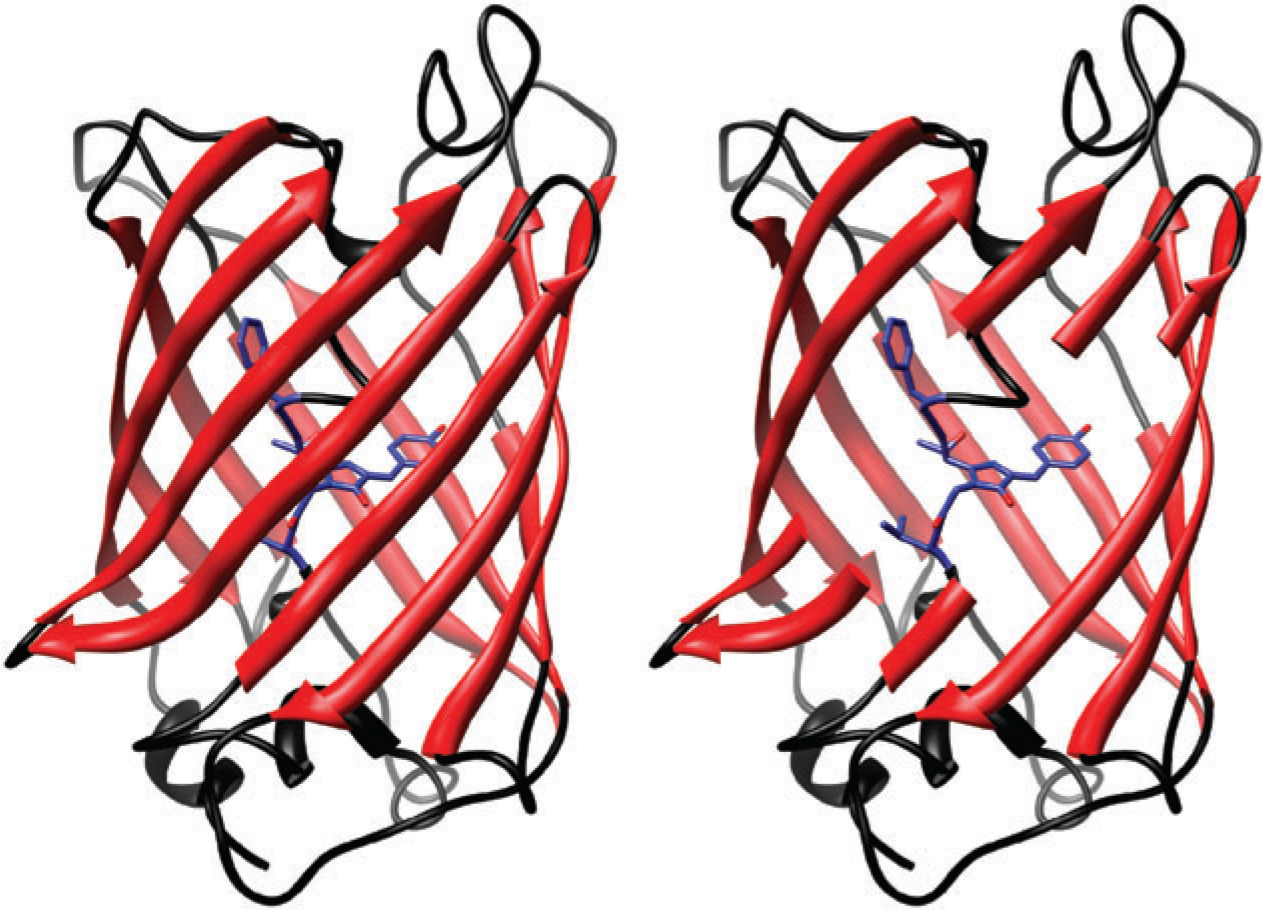

Fig. 1.
Green fluorescent protein crystal structure as ribbon diagram (left), and as cut-away showing encapsulated chromophore. Protein Data Bank entry 1EMA.

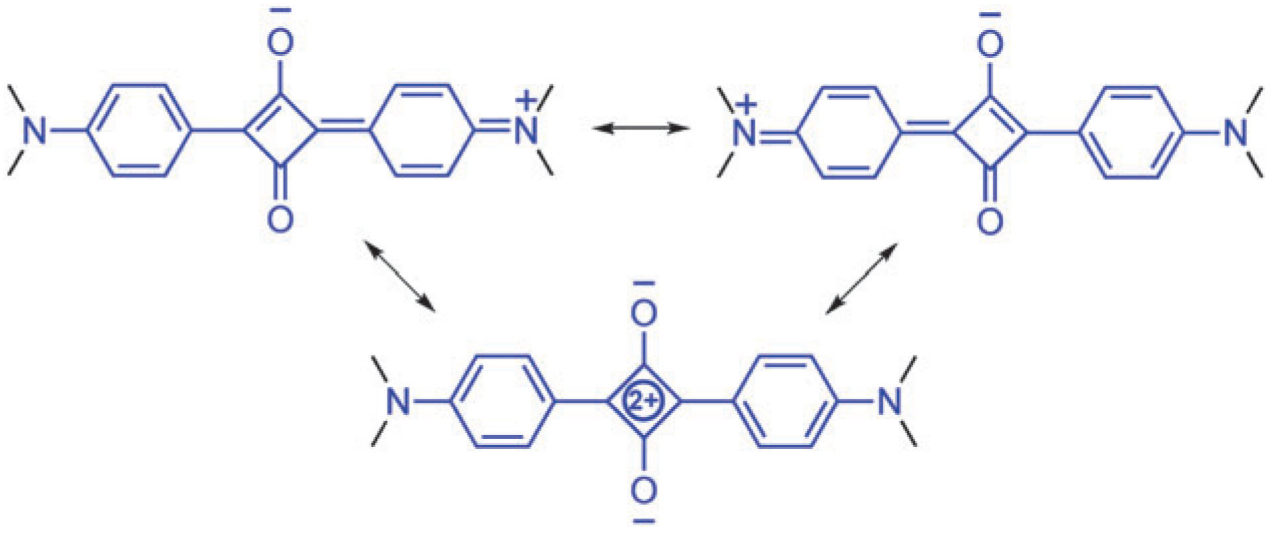

Fig. 2.
Squaraine resonance structures.

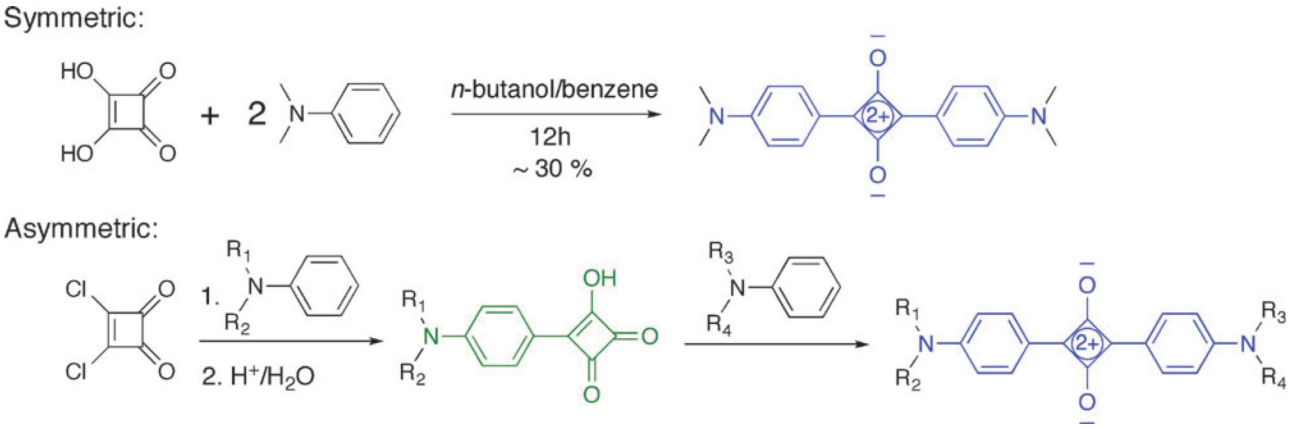

Scheme 1.
Synthesis of squaraine dyes.

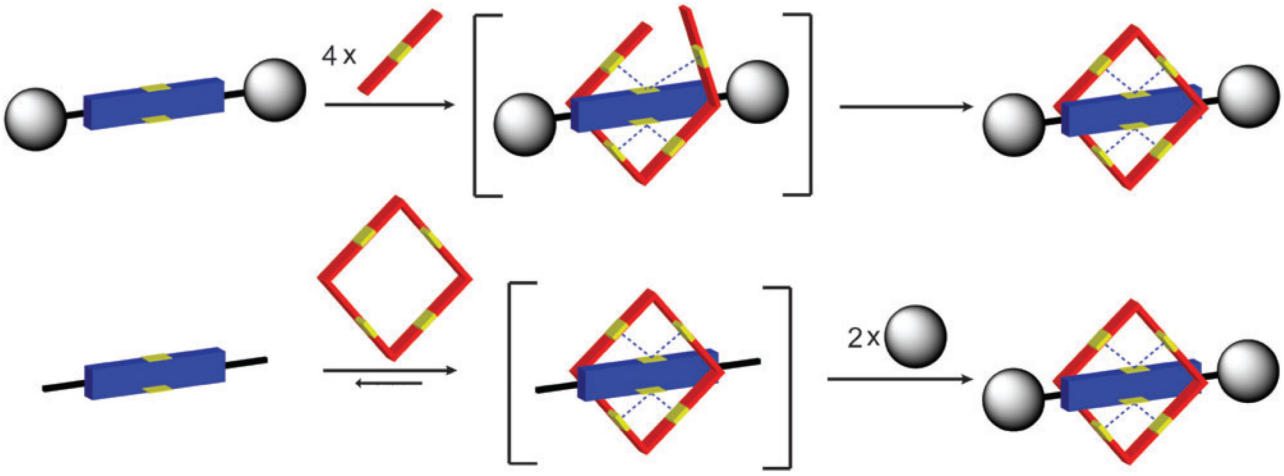

Fig. 3.
Rotaxane synthesis by clipping reaction (top) and capping reaction (bottom).

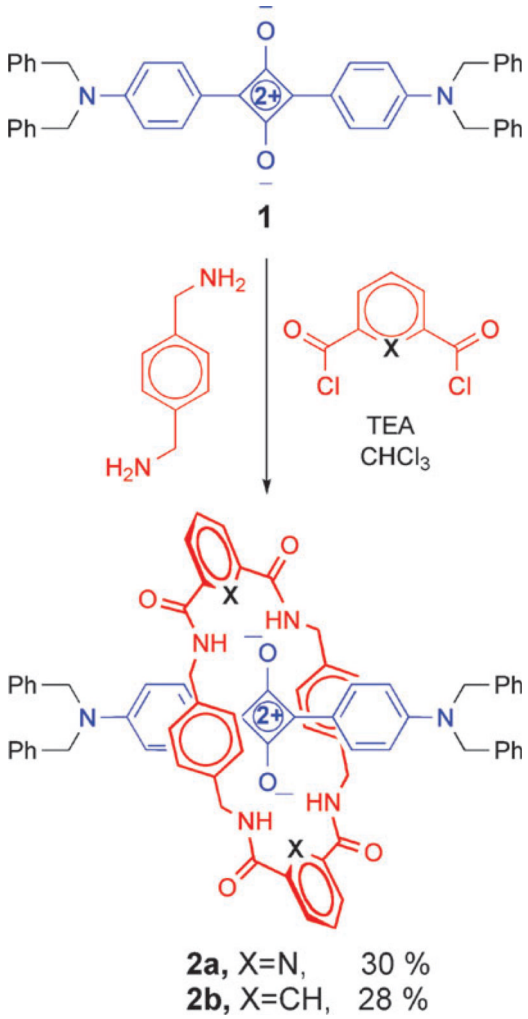

Scheme 2.
Synthesis of first-generation squaraine rotaxanes using Leigh-type clipping reaction.

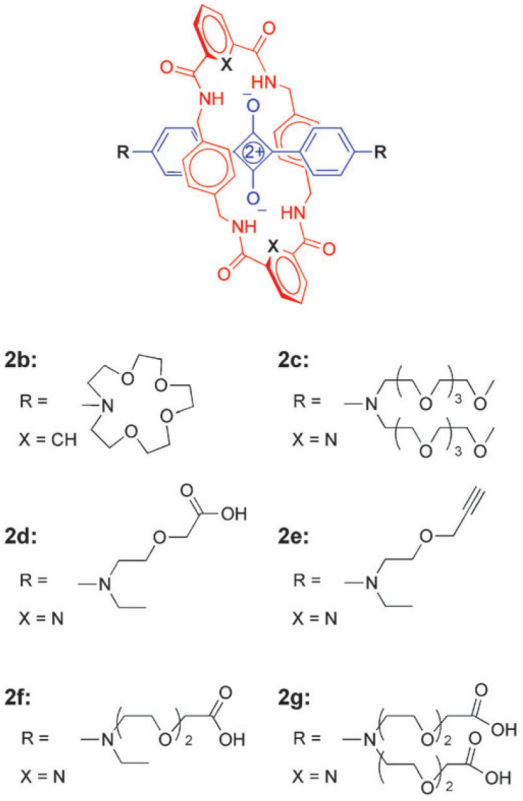

Fig. 4.
Squaraine rotaxanes with different stopper groups.

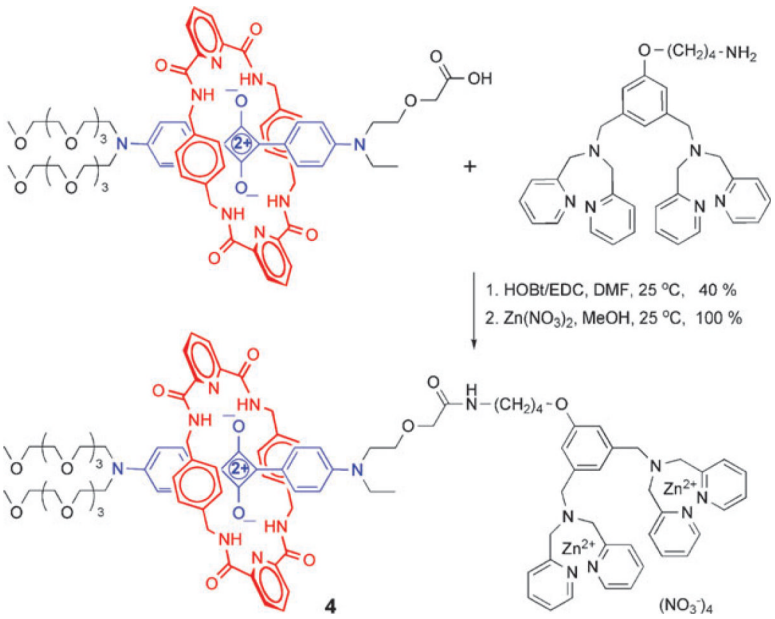

Scheme 3.
Synthesis of squaraine rotaxane bis-ZnDPA conjugate **4**.

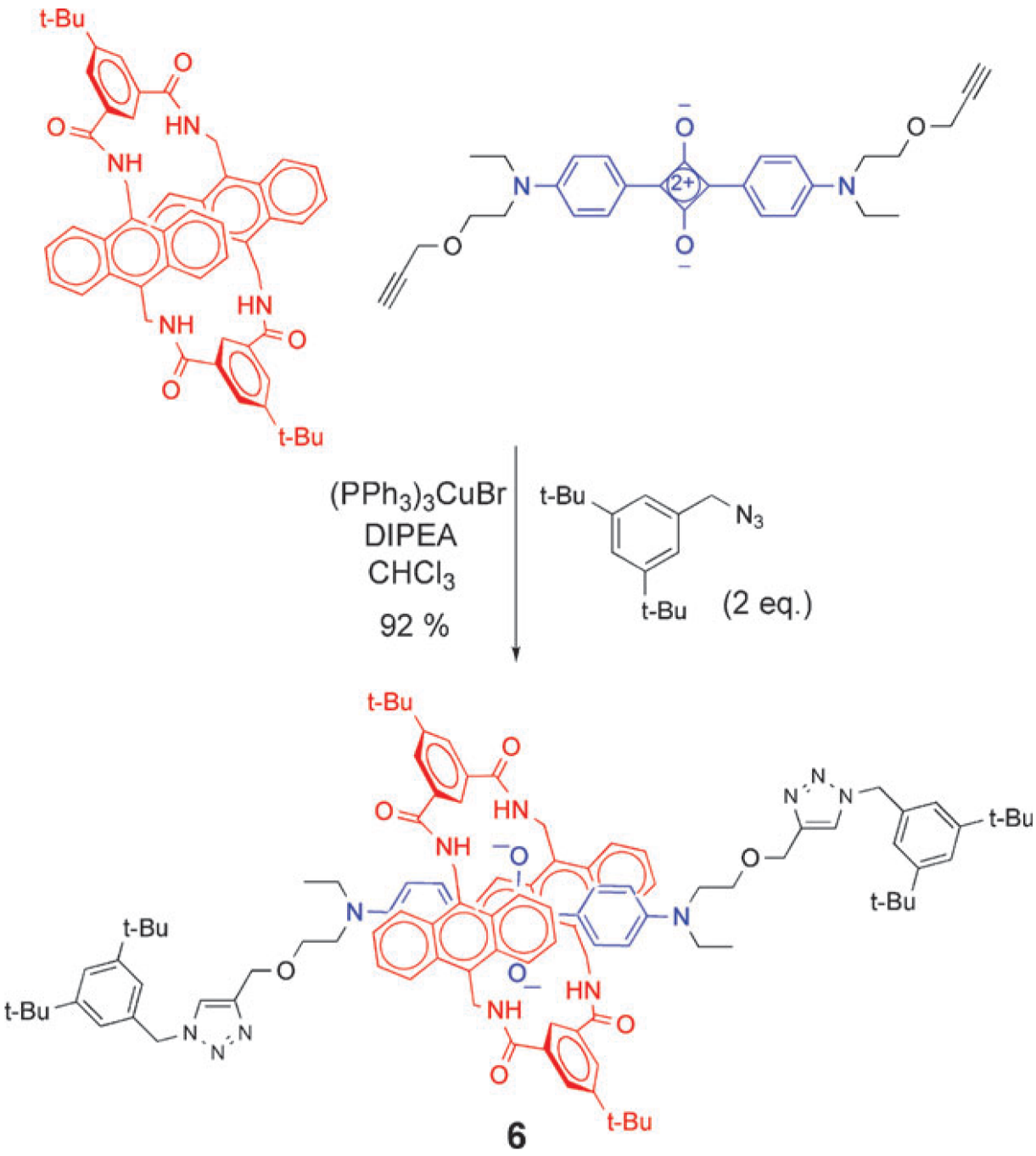

Scheme 4.
Capping reaction to form squaraine rotaxane **6**.

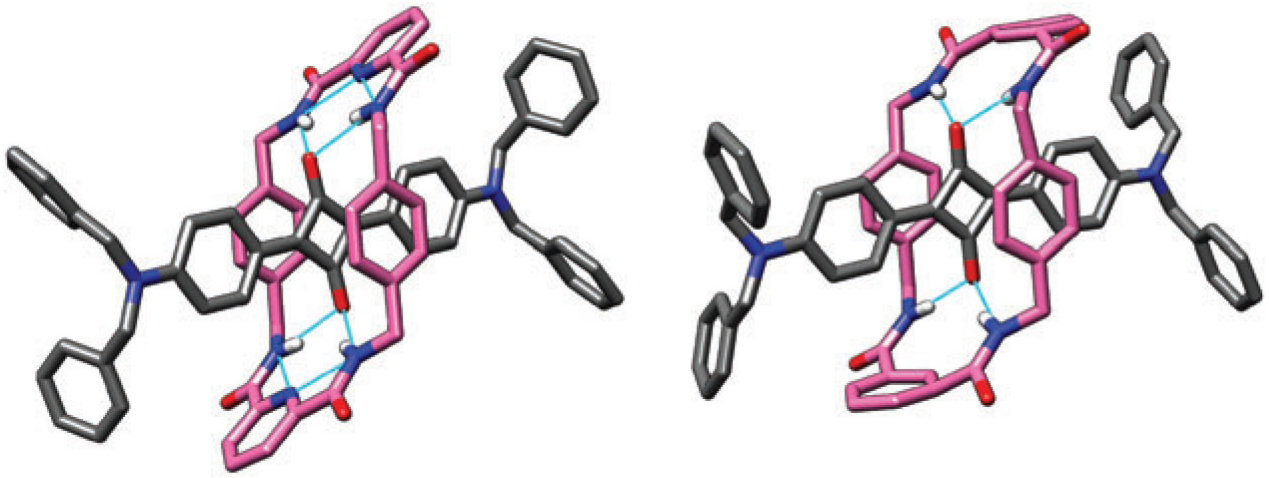

Fig. 5.
X-Ray crystal structures of pyridyl-containing rotaxane **2a** (left) and of isophthalamide-containing rotaxane **2b** (right).

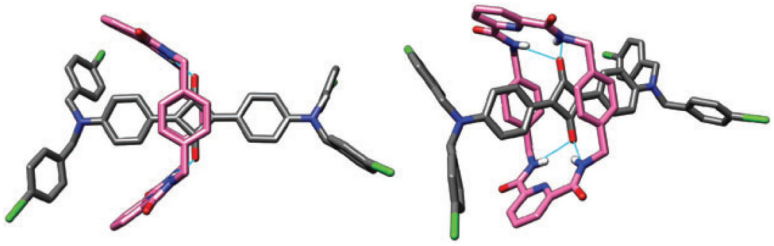

Fig. 6.
Two views of the X-ray crystal structure of squaraine rotaxane **7**.

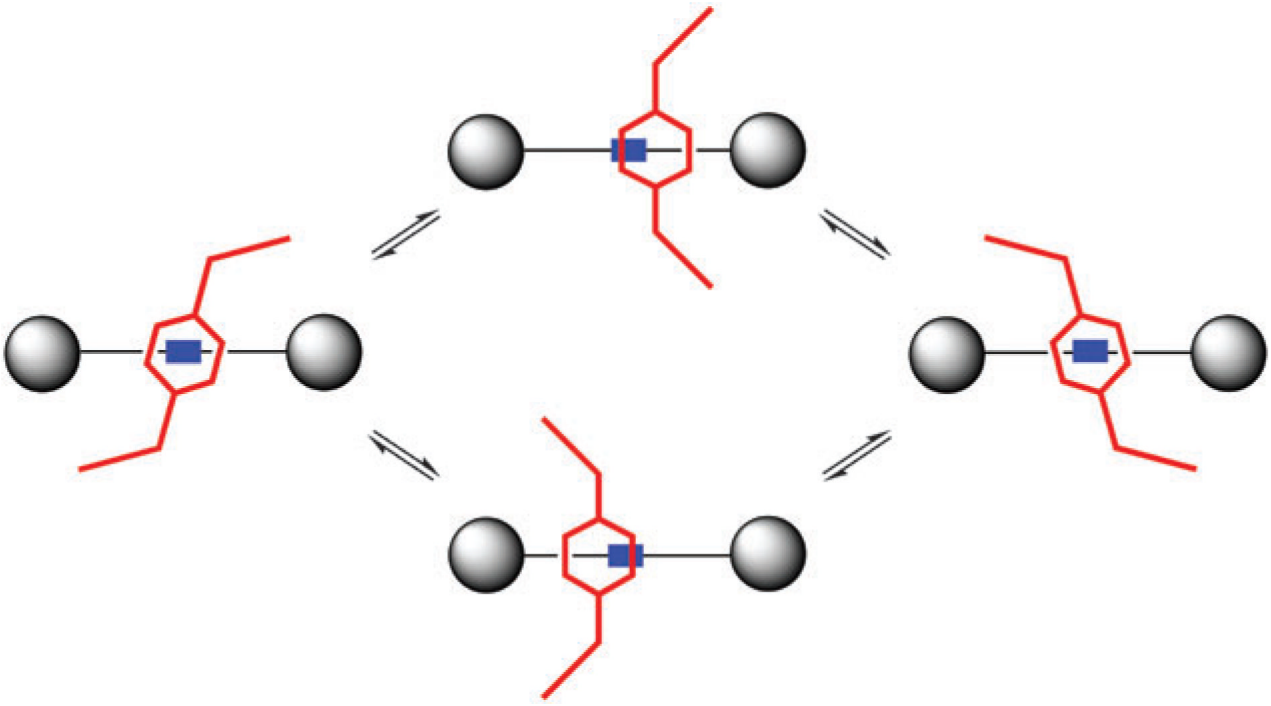

Fig. 7.
Macrocycle chair/boat conformation for squaraine rotaxanes.

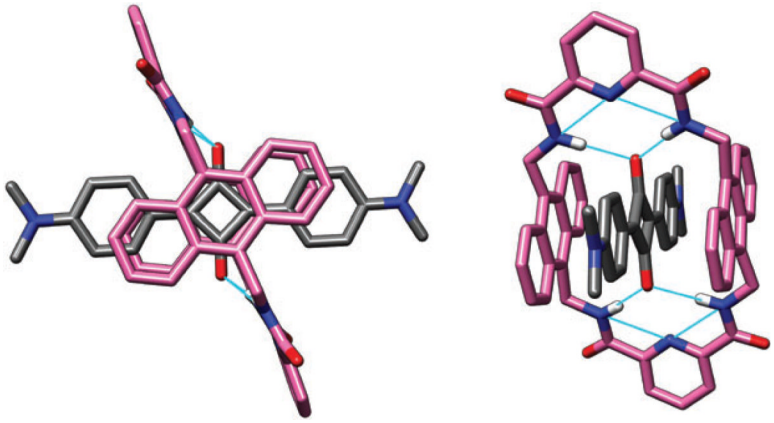

Fig. 8.
Two views of the X-ray crystal structure of *N*,*N*′-tetramethylsquaraine encapsulated by macrocycle **5a**.

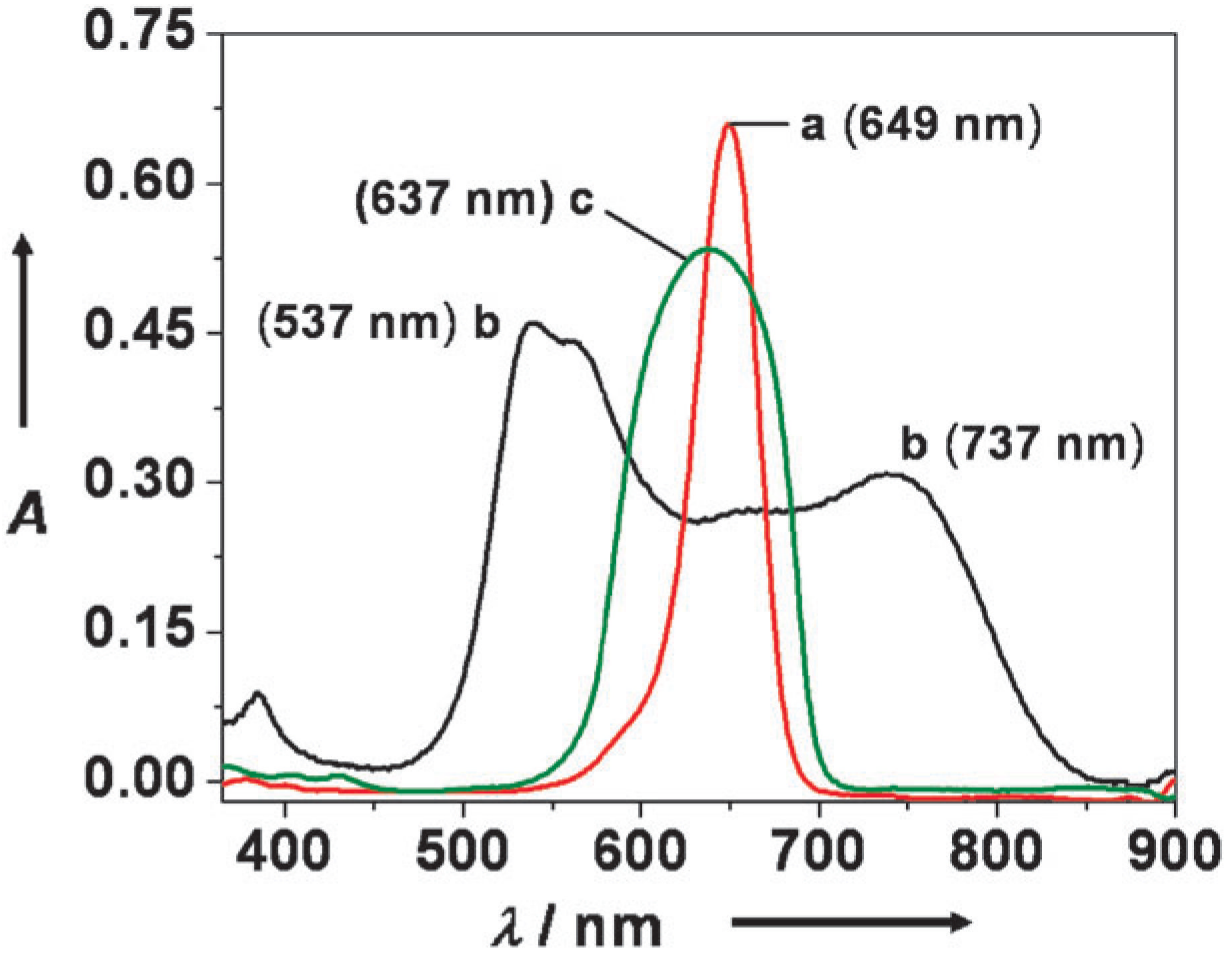

Fig. 9.
Absorption spectra of squaraine **1** in DMSO (a), squaraine **1** in 1 : 1 DMSO–H_2O (b), and rotaxane **2a** in 9 : 1 DMSO–H_2O (c). Reproduced with permission from ref. [13]. Copyright 2005, American Chemical Society.

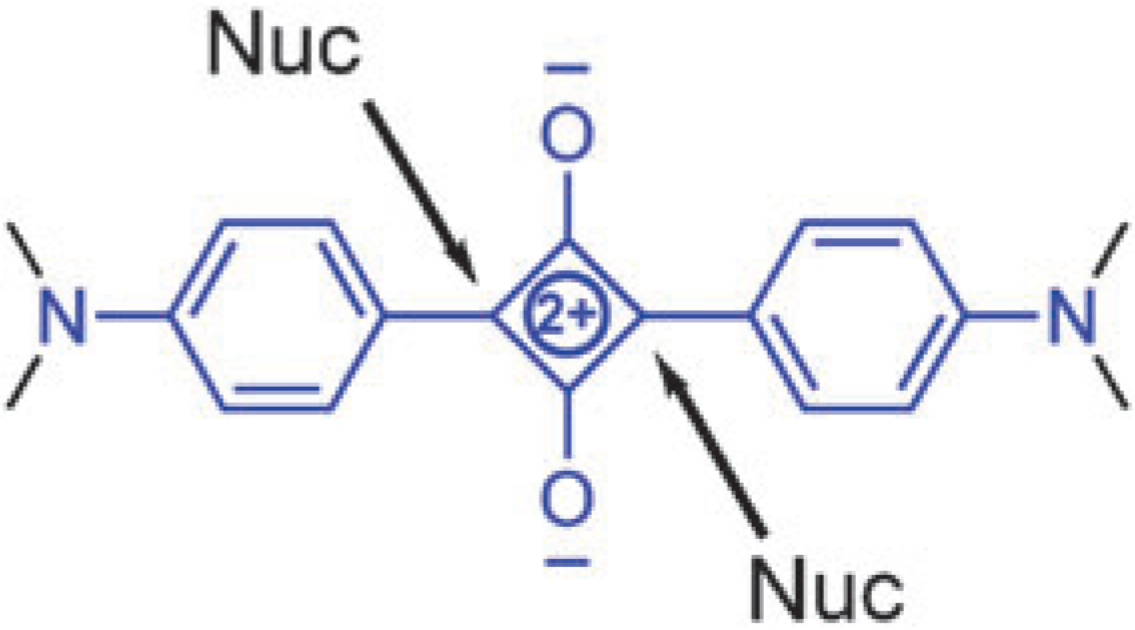

Fig. 10.
Sites of nucleophilic attack.

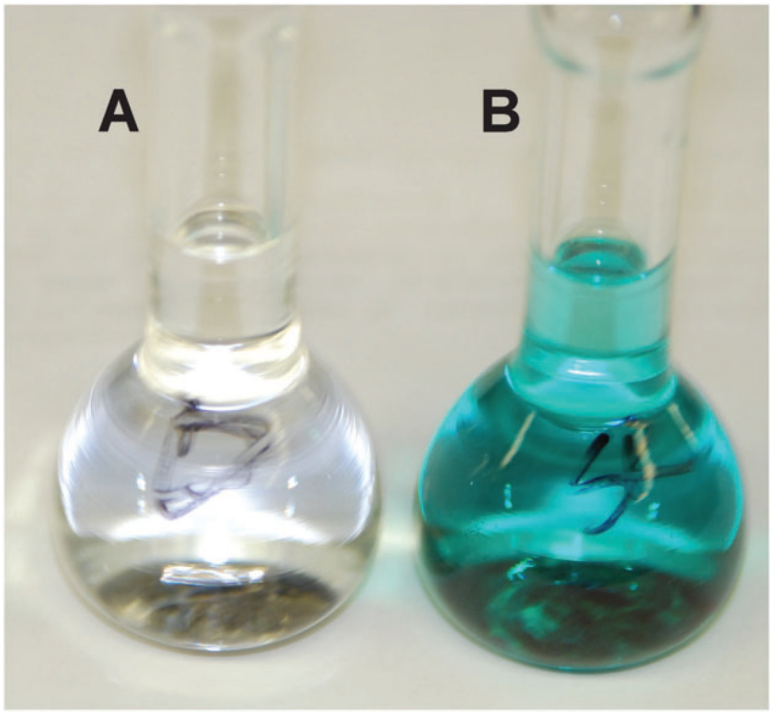

Fig. 11.
Addition of excess cysteine to solution of squaraine **1** induces loss of color within five minutes (A), whereas the same addition to squaraine rotaxane **2a** has no effect (B).

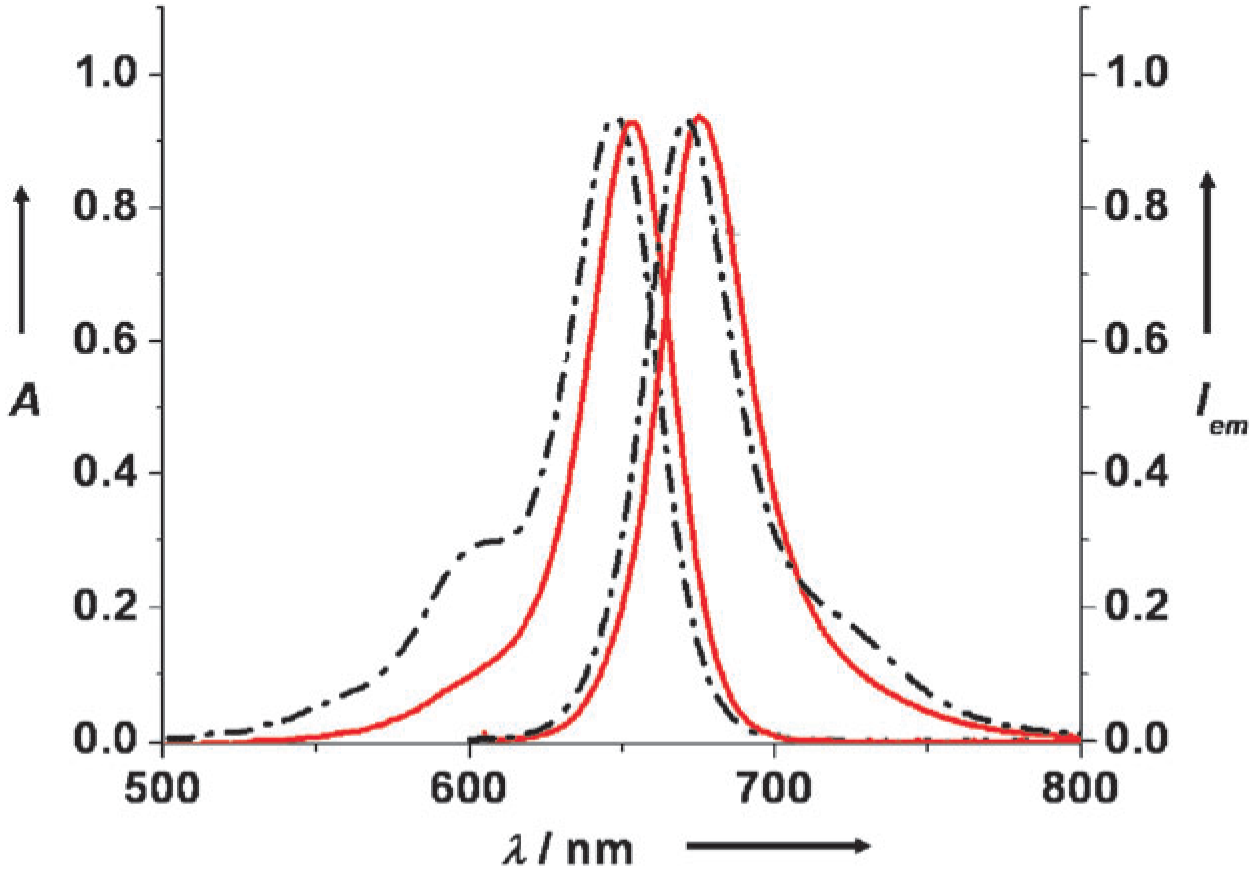

Fig. 12.
Absorption and emission maxima for squaraine rotaxane **8** (red) and cyanine **9** (black). Reproduced with permission from ref. [21]. Copyright Wiley-VCH Verlag GmbH & Co. KGaA.

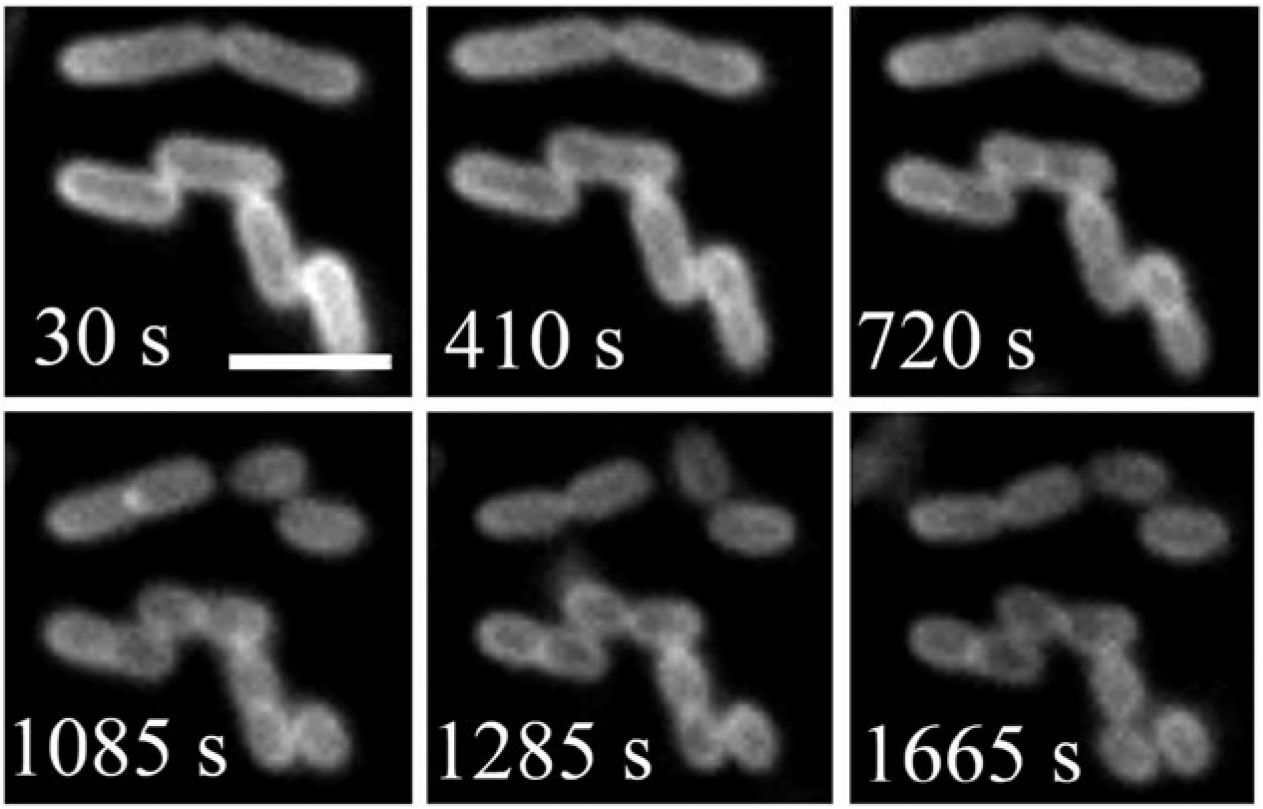

Fig. 13.
Binary fission of *E. coli* cells stained with probe **8**. The cells were imaged every 5 s for 30 min by using fluorescence microscopy. The scale bar represents 2 μm. Reproduced with permission from ref. [21]. Copyright Wiley-VCH Verlag GmbH & Co. KGaA.

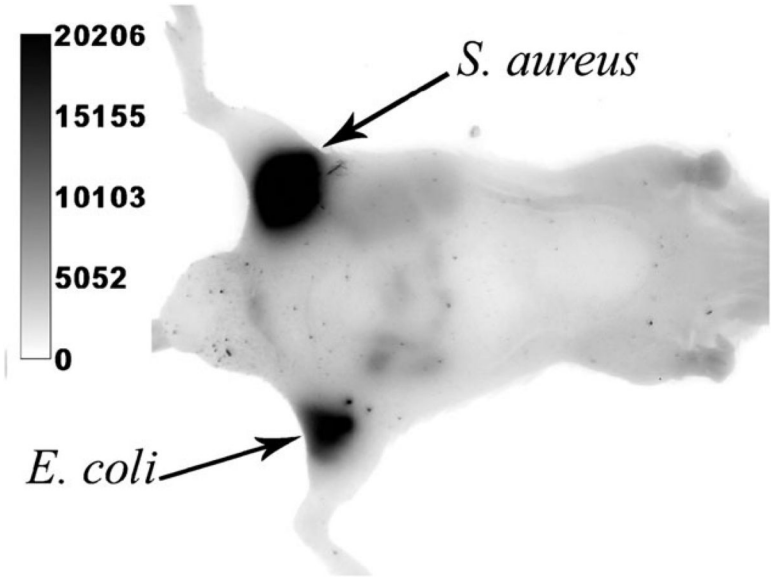

Fig. 14.
Fluorescence optical imaging of a live nude mouse with separate subcutaneous injections of *S. aureus* and *E. coli* that were prelabeled with **8**. Reproduced with permission from ref. [21]. Copyright Wiley-VCH Verlag GmbH & Co. KGaA.

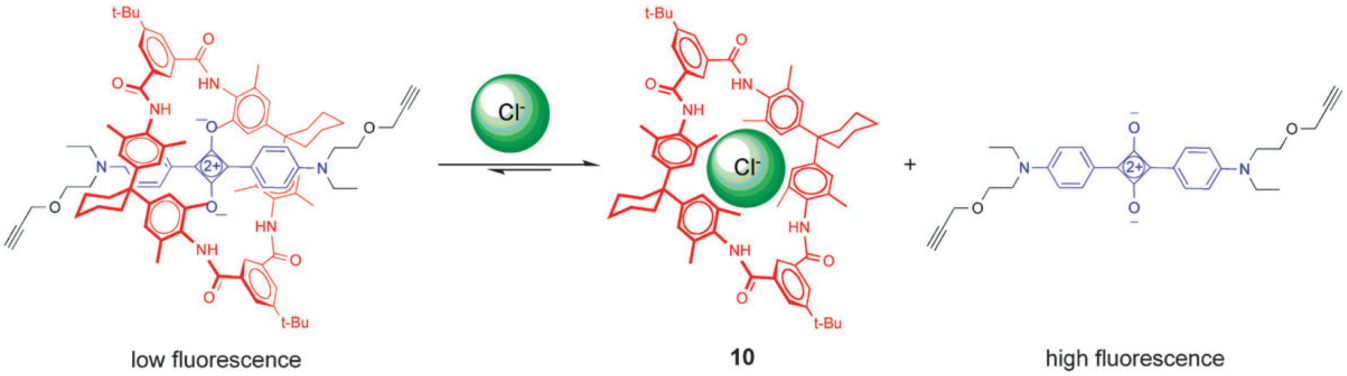

Fig. 15.
Cl^- displaces squaraine dye from quenching tetralactam macrocycle **10**.

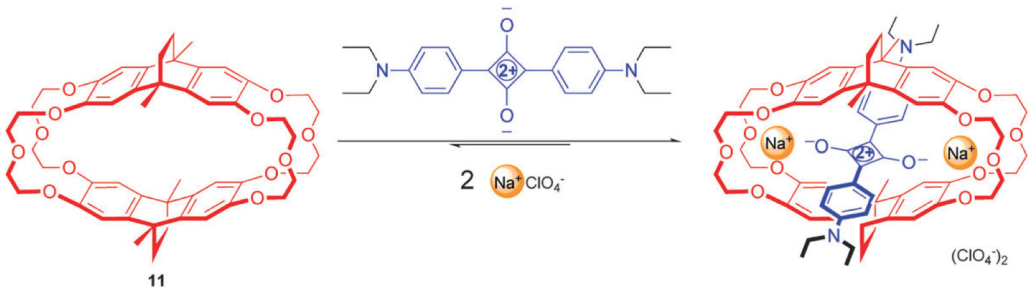

Fig. 16.
Crown ether cyclophane **11** encapsulates squaraine dye only in the presence of Na^+. Reproduced with permission from ref. [48]. Copyright Wiley-VCH Verlag GmbH & Co. KGaA.

Table 1

Photophysical properties of squaraine rotaxane derivatives

Compound	Solvent	λ_{abs}/nm	λ_{em}[a]/nm	Φ_f[b]
1	THF	631	650	0.61
2a	THF	639	659	0.70
	THF–H_2O (4 : 1)	643	667	0.58
2b	THF–H_2O (4 : l)	650	676	0.15
3	THF	644	672	0.61
4	H_2O	650	669	0.08
6	$CHCl_3$	661	704[c]	0.47
7	THF	638	657	0.74
8	H_2O	653	675	0.20

[a] Solutions were excited at 590 nm and emission monitored in the region 600–750 nm for estimating Φ_f.

[b] Fluorescence quantum yields were determined using 4,4-[bis(*N*,*N*-dimethylamino)phenyl]squaraine dye as the standard (Φ_f = 0.70 in $CHCl_3$), error limit ±5%.

[c] Solution was excited at 605 nm and emission monitored in the region 620–850 nm for estimating Φ_f.